Composite Structures 27 (1994) 403–418

Geometrically non-linear analysis of symmetrically laminated composite and sandwich shells with a higher-order theory and C^0 finite elements

T. Kant & J. R. Kommineni

Department of Civil Engineering, Indian Institute of Technology, Powai, Bombay-400076, India

A C^0 continuous displacement based finite element formulation of a higher-order theory for linear and geometrically non-linear analysis (which accounts for large displacements in the sense of von Karman) of symmetrically laminated composite and sandwich shells under transverse loads is presented. The displacement model accounts for non-linear and constant variation of tangential and transverse displacement components, respectively, through the shell thickness. The assumed displacement model eliminates the use of shear correction coefficients. The discrete element chosen is a nine-node quadrilateral element with nine degrees of freedom per node. The accuracy of the present formulation is then established by comparing the present results with the available analytical closed-form two-dimensional solutions, three-dimensional elasticity solutions and other finite element solutions. Some new results are generated for future comparisons to and evaluations of sandwich shells.

1 INTRODUCTION

Structural elements made up of fibre reinforced composite materials have been extensively used in high and low technology areas in recent years. Their industrial applications are multiplying rapidly because of their superior mechanical properties. However, the engineering community is faced with many challenging problems associated with the use of these new materials. Of these, the geometric non-linear response of laminated shells is one of the major considerations in their design.

An accurate prediction of the behaviour of shell structures requires modelling of actual geometry and kinematic description of the components. The partial differential equations describing the large deflection behaviour of anisotropic composite shells of arbitrary geometry are not amenable to classical analytical methods. The finite element method has proved to be a very powerful tool for analyzing structural problems, involving complex geometries, loadings, boundaries and non-linearities.

Many classical theories were developed originally for thin elastic shells and are based on Love–Kirchhoff assumptions, and surveys of such classical shell theories can be seen in the works of Naghdi[1] and Bert.[2]

The first analysis that incorporated the bending and stretching coupling is that of Ambartsumyan.[3,4] Ambartsumyan assumed that the individual orthotropic layers were oriented such that the principal axes of material symmetry coincided with that of the principal coordinates of the shell reference surface. The effects of transverse shear deformation, normal stress and normal strain on the behaviour of laminated shells can be incorporated on the basis of a mathematical model through the inclusion of higher-order terms in the power series expansion of the assumed displacement field. In the context of a special orthotropic and homogeneous shells, Hildebrand *et al.*[5] were the first to make significant contributions by dispensing with all the Love assumptions and assuming a three-term Taylor's series expansion for the displacement vector. Naghdi[6] has employed Reissner's[7] mixed variational principle to develop a complete shell formulation similar to that of Hildebrand *et al.* Dong and Tso[8] were perhaps the first to present a first-order shear

Composite Structures 0263-8223/94/$07.00

deformation theory (which includes the effects of transverse shear deformation through the shell thickness) and then to construct a laminated orthotropic shell theory. Further attempts at refining theories for laminated anisotropic cylindrical shells have been presented by Whitney and Sun[9] and Widera and Logan.[10] Reddy[11] extended Sander's theory for simply supported cross-ply laminated shells.

The second-order transverse shear deformation effects have been included by Kant,[12] who developed a complete governing set of equations for a thick shell theory. The theory is based on a three-term Taylor's series expansion of the displacement vector and generalized Hooke's law, and is applicable to orthotropic material laminae having planes of symmetry coincident with shell coordinates. Kant and Ramesh[13] have presented a general orthotropic shell theory in orthogonal curvilinear coordinates based on a displacement model of Hildebrand *et al.* Kant[14,15] presented higher-order theories for general orthotropic as well as laminated shells, which are derived from the three-dimensional elasticity equations by expanding the displacement vector in Taylor's series in the thickness coordinate. The theories account for the effects of transverse shear deformation, transverse normal stress and transverse normal strain with an implicit non-linear distribution of the tangential displacement components through the shell thickness.

Reddy and Liu[16] presented a higher-order theory for doubly curved shells and used Navier's approach for solution. Bhimaraddi and Stevens[17] and Murthy and Reddy[18] presented higher-order displacement based shear deformation theories based on C^1 continuity. Kant and Pandya[19] presented different higher-order shear deformation theories for static analysis of laminated composite plates using C^0 continuity. Kant and Menon[20–22] presented various higher-order theories for laminated composite cylindrical shells using C^0 finite elements. Kant[20–31] along with co-workers, after doing extensive numerical investigations on laminated plates and shells, both static and dynamic linear analysis, using C^0 finite elements and various higher-order theories, proved that shear-free conditions at bounding planes give stiffer solutions; and he also proved that among various displacement models, for flat laminates, the one which has nine degrees of freedom per node gives results very close to 3D elasticity solution (e.g. Kant and Pandya[19]). As regards curved laminates, the work is under progress and a definite conclusion will emerge after further work.

Kabir[32] presented an analytical solution to the boundary value problems of static and dynamic responses of cross-ply and arbitrarily laminated doubly curved shells of rectangular plan form. Three novel solution methods are proposed based on double Fourier series.

First, a boundary discontinuous double Fourier series method is adopted to solve the static and eigenvalue problems of cross-ply and angle-ply laminated doubly curved shells based on classical lamination theory and static problems of cross-ply laminated doubly curved shells based on higher-order shear deformation theory. Then a general boundary discontinuous double Fourier series method and a boundary continuous double Fourier series method are described to solve static and eigenvalue problems of cross-ply laminated doubly curved shells and static problems of anti-symmetric angle-ply laminated doubly curved shells based on a first-order shear deformation theory. However, little attention is focused on the higher-order theory. All of these studies are limited to small deformation theory.

Because of the high modulus and high strength properties of composites, structural composites undergo large deformations before they become inelastic. Therefore, an accurate prediction of displacements and stresses are possible only when one accounts for the geometric non-linearity. Horrigmoe and Bergan[33] presented classical variational principles for non-linear problems by considering incremental deformations of a continuum. Wunderlich[34] and Stricklin *et al.*[35] have reviewed various principles of incremental analysis and solution procedures for non-linear problems, respectively.

Noor and Hartley[36] employed the shallow shell theory with transverse shear strains and geometric non-linearities to develop triangular and quadrilateral finite elements. Chang and Sawamiphakdi[37] presented a formulation of the degenerate 3D shell element for geometrically non-linear analysis of laminated composite shells. The updated incremental formulation does not include any numerical results for laminated shells.

Chao and Reddy[38] and Reddy and Chandrashekhara[39] have presented first-order shear deformation theory by including transverse shear strains effects in Sander's theory for geometrically non-linear analysis of doubly curved shells. Recently, Kant and Mallikarjuna[27] presented a

geometrically non-linear dynamic response of laminated plates with a higher-order theory and C^0 finite elements.

To the authors' knowledge there is no published work on higher-order shear deformation theory including the geometric non-linearity with C^0 finite elements. In this paper, a third-order shear deformation theory is constructed in which the tangential displacement components are a cubic function of z, whereas the transverse displacement component is assumed to be constant through the thickness of the shell. The effect of geometric non-linearity is included in the formulation by adopting the von Karman assumptions (see Chao and Reddy[35] and Reddy and Chandrashekhara[39]). That is, the first derivatives of tangential displacement components with respect to x, y and z are small in comparison to the first derivatives of the transverse displacement component with respect to x, y and z.

In the present investigation, a C^0 nine-node bi-quadratic Lagrangian finite element has been adopted in the numerical computations. In addition to the higher-order shear deformation theory, a first-order shear deformation theory by including first-order shear deformation effects into Sander's shell theory (see Sanders[37]) is developed so as to enable a comparison of the present formulation with a parallel formulation. Several examples drawn from the literature are analyzed and appropriate comparisons are made to show the simplicity, validity and accuracy of the present formulation.

2 THEORY AND FORMULATION

A fibre reinforced composite general shell is presented which consists of homogeneous and isotropic/orthotropic layers of thicknesses h_1, h_2, h_3, ... h_{NL}, oriented arbitrarily such that the total thickness $h = h_1 + h_2 + \ldots + h_{NL}$, where NL stands for total number of layers in the laminate. The x, y are the curvilinear dimensional coordinates defining the mid-surface of the shell and the z axis is oriented in the thickness direction (Fig. 1).

In the present theory the displacement components of a generic point in the shell are assumed to be of the following form:

$$\begin{aligned} u(x, y, z) &= u_0(x, y) + z\,\theta_1(x, y) + z^2 u_0^*(x, y) + z^3 \theta_1^*(x, y) \\ v(x, y, z) &= v_0(x, y) + z\,\theta_2(x, y) + z^2 v_0^*(x, y) + z^3 \theta_2^*(x, y) \\ w(x, y, z) &= w_0(x, y) \end{aligned} \tag{1}$$

where u_0, v_0 and w_0 are mid-surface displacements of a generic point having displacements u, v, w in the x, y and z directions, respectively; θ_1 and θ_2 are rotations of the transverse normal cross-sections in the xz and yz planes, respectively; u_0^*, v_0^*, θ_1^* and θ_2^* are the corresponding higher-order terms in the Taylor's series expansion and the mid-surface displacement components u_0, v_0, w_0, θ_1, θ_2, u_0^*, v_0^*, θ_1^*, θ_2^* are the nine degrees of freedom of the present higher-order displacement model.

The present theory considers large displacements in the sense of von Karman with small strains, which in particular imply that the first-order derivatives of tangential displacement components with respect to x, y and z are small, so that their particular products can be neglected (see Novozhilov[21], Chao and Reddy[35] and Reddy and Chandrashekhara[39]). The following are the strain–displacement relations

$$\begin{aligned} \varepsilon_x &= \frac{\partial u}{\partial x} + \frac{w}{R_1} + \frac{1}{2}\cdot\left(\frac{\partial w}{\partial x}\right)^2 \\ \varepsilon_y &= \frac{\partial v}{\partial y} + \frac{w}{R_2} + \frac{1}{2}\cdot\left(\frac{\partial w}{\partial y}\right)^2 \\ \gamma_{xy} &= \frac{\partial u}{\partial y} + \frac{\partial v}{\partial x} + \frac{\partial w}{\partial x}\cdot\frac{\partial w}{\partial y} \\ \gamma_{xz} &= \frac{\partial u}{\partial z} + \frac{\partial w}{\partial x} - \frac{u}{R_1} \\ \gamma_{yz} &= \frac{\partial v}{\partial z} + \frac{\partial w}{\partial y} - \frac{v}{R_2} \end{aligned} \tag{2}$$

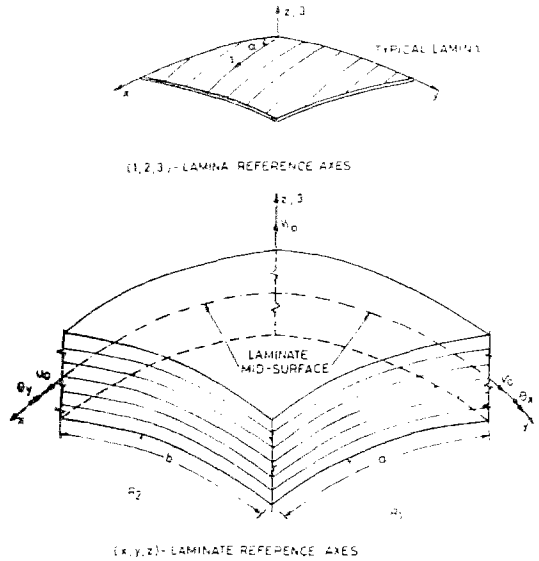

Fig. 1. Laminate geometry with positive set of lamina/laminate reference axes, displacement components and fibre orientation.

Upon substituting displacement components given by eqns (1) in eqn (2) and simplifying, the strain components in terms of mid-surface displacement components are obtained as follows:

$$\varepsilon_x = \frac{\partial u_0}{\partial x} + \frac{w_0}{R_1} + z\cdot\frac{\partial \theta_x}{\partial x} + z^2\cdot\frac{\partial u_0^*}{\partial x} + z^3\cdot\frac{\partial \theta_x^*}{\partial x} + \frac{1}{2}\cdot\left(\frac{\partial w_0}{\partial x}\right)^2$$

$$\varepsilon_y = \frac{\partial v_0}{\partial y} + \frac{w_0}{R_2} + z\cdot\frac{\partial \theta_y}{\partial y} + z^2\cdot\frac{\partial v_0^*}{\partial y} + z^3\cdot\frac{\partial \theta_y^*}{\partial y} + \frac{1}{2}\cdot\left(\frac{\partial w_0}{\partial y}\right)^2$$

$$\gamma_{xy} = \left(\frac{\partial v_0}{\partial x} + \frac{\partial u_0}{\partial y}\right) + z\cdot\left(\frac{\partial \theta_x}{\partial x} + \frac{\partial \theta_y}{\partial y}\right) + z^2\cdot\left(\frac{\partial v_0^*}{\partial x} + \frac{\partial u_0^*}{\partial y}\right) + z^3\cdot\left(\frac{\partial \theta_x^*}{\partial x} + \frac{\partial \theta_y^*}{\partial y}\right) + \frac{\partial w_0}{\partial x}\cdot\frac{\partial w_0}{\partial y} \tag{3}$$

$$\gamma_{xz} = \left(\theta_x + \frac{\partial w_0}{\partial x} - \frac{u_0}{R_1}\right) + z\cdot\left(2u_0^* - \frac{\theta_x}{R_1}\right) + z^2\cdot\left(3\theta_x^* - \frac{u_0^*}{R_1}\right) + z^3\cdot\left(-\frac{\theta_x^*}{R_1}\right)$$

$$\gamma_{yz} = \left(\theta_y + \frac{\partial w_0}{\partial y} - \frac{v_0}{R_2}\right) + z\cdot\left(2v_0^* - \frac{\theta_y}{R_2}\right) + z^2\cdot\left(3\theta_y^* - \frac{v_0^*}{R_2}\right) + z^3\cdot\left(-\frac{\theta_y^*}{R_2}\right)$$

The constitutive equations of the lth layer can be written as:

$$\begin{bmatrix}\sigma_1\\ \sigma_2\\ \tau_{12}\\ \tau_{13}\\ \tau_{23}\end{bmatrix}^l = \begin{bmatrix} C_{11} & C_{12} & 0 & 0 & 0\\ & C_{22} & 0 & 0 & 0\\ & & C_{33} & 0 & 0\\ \text{Symmetric} & & & C_{44} & 0\\ & & & & C_{55}\end{bmatrix}^l \begin{bmatrix}\varepsilon_1\\ \varepsilon_2\\ \gamma_{12}\\ \gamma_{13}\\ \gamma_{23}\end{bmatrix}^l \tag{4a}$$

where $(\sigma_1, \sigma_2, \tau_{12}, \tau_{13}, \tau_{23})$ are the stress components and $(\varepsilon_1, \varepsilon_2, \gamma_{12}, \gamma_{13}, \gamma_{23})$ are the strain components referred to the lamina coordinates $(1, 2, 3)$ as shown in Fig. 1 and C_{ij} are the composite material stiffness matrix coefficients of the Lth lamina in lamina axes $(1, 2, 3)$ and these are defined as follows:

$$C_{11} = \left(\frac{E_1}{1 - \nu_{12}\nu_{21}}\right); \quad C_{12} = \left(\frac{\nu_{12}E_2}{1 - \nu_{12}\nu_{21}}\right)$$

$$C_{22} = \left(\frac{E_2}{1 - \nu_{12}\nu_{21}}\right); \quad C_{33} = G_{12}; \quad C_{44} = G_{13} \tag{4b}$$

$$C_{55} = G_{23}$$

Through a tensor transformation, the stress strain relations of the Lth lamina of a cross-ply laminate in the laminate coordinates (x, y, z) can be written as:

$$\boldsymbol{\sigma} = \boldsymbol{Q}\boldsymbol{\varepsilon} \tag{5a}$$

$$\begin{bmatrix} \sigma_x \\ \sigma_y \\ \tau_{xy} \\ \tau_{yz} \\ \tau_{xz} \end{bmatrix}^L = \begin{bmatrix} Q_{11} & Q_{12} & 0 & 0 & 0 \\ & Q_{22} & 0 & 0 & 0 \\ & & Q_{33} & 0 & 0 \\ \text{Symmetric} & & & Q_{44} & 0 \\ & & & & Q_{55} \end{bmatrix}^L \begin{bmatrix} \varepsilon_x \\ \varepsilon_y \\ \gamma_{xy} \\ \gamma_{yz} \\ \gamma_{xz} \end{bmatrix}^L \tag{5b}$$

in which $\boldsymbol{\sigma}^L = (\sigma_x, \sigma_y, \tau_{xy}, \tau_{yz}, \tau_{xz})$ and $\boldsymbol{\varepsilon}^L = (\varepsilon_x, \varepsilon_y, \gamma_{xy}, \gamma_{yz}, \gamma_{xz})$ are the stress and strain vectors with respect to the laminate axes (x, y, z) and the coefficients of matrix $\boldsymbol{Q}$ corresponding to the Lth lamina are defined as follows:

$$\begin{aligned} Q_{11} &= C_{11} \cdot c^4 + C_{22} \cdot s^4 \\ Q_{12} &= C_{12} \cdot c^2 + s^2 \\ Q_{22} &= C_{11} \cdot s^4 + C_{22} \cdot c^4 \\ Q_{33} &= C_{33} \cdot c^2 + s^2 \\ Q_{44} &= C_{44} \cdot c^2 + C_{55} \cdot s^2 \\ Q_{55} &= C_{44} \cdot s^2 + C_{55} \cdot c^2 \end{aligned} \tag{5c}$$

where $c = \cos\theta$, $s = \sin\theta$, θ is the angle between fibre direction of the lamina and the x axis of the laminate.

The total potential energy of the system (Π) is given by:

$$\Pi = \frac{1}{2} \times \int_V \boldsymbol{\varepsilon}^L \cdot \boldsymbol{\sigma}\, \mathrm{d}V - \int_A \boldsymbol{d}^L \cdot \boldsymbol{F}\, \mathrm{d}A \tag{6}$$

$$\Pi = \frac{1}{2} \times \int_A \left(\int \boldsymbol{\varepsilon}^L \cdot \boldsymbol{\sigma}\, \mathrm{d}z \right) \mathrm{d}A - \int_A \boldsymbol{d}^L \cdot \boldsymbol{F}\, \mathrm{d}A \tag{7}$$

in which A is the mid-surface area, V is the shell volume, $\boldsymbol{F}$ is the equivalent load vector corresponding to nine degrees of freedom $\boldsymbol{d}$, i.e. $\boldsymbol{d}^L = (u_0, v_0, w_0, \theta_x, \theta_y, u_0^*, v_0^*, \theta_x^*, \theta_y^*)$.

The expressions for the strain components given by eqn (3) are substituted in eqn (7). The function given by eqn (7) is then minimized whilst carrying out explicit integration through the shell thickness. This

leads to a stress resultant vector $\bar{\sigma}$ whose components for an NL layered laminated shell are defined as follows:

$$[\boldsymbol{N}, \boldsymbol{N}^*] = \begin{bmatrix} N_x & N_x^* \\ N_y & N_y^* \\ N_{xy} & N_{xy}^* \end{bmatrix} = \sum_{l=1}^{NL} \int_{z_l}^{z_{l+1}} \begin{bmatrix} \sigma_x \\ \sigma_y \\ \tau_{xy} \end{bmatrix} [1, z^2] \, dz$$

$$[\boldsymbol{M}, \boldsymbol{M}^*] = \begin{bmatrix} M_x & M_x^* \\ M_y & M_y^* \\ M_{xy} & M_{xy}^* \end{bmatrix} = \sum_{l=1}^{NL} \int_{z_l}^{z_{l+1}} \begin{bmatrix} \sigma_x \\ \sigma_y \\ \tau_{xy} \end{bmatrix} [z, z^3] \, dz \tag{8}$$

$$[\boldsymbol{Q}, \boldsymbol{Q}^*, \boldsymbol{S}, \boldsymbol{S}^*] = \begin{bmatrix} Q_x & Q_x^* & S_x & S_x^* \\ Q_y & Q_y^* & S_y & S_y^* \end{bmatrix} = \sum_{l=1}^{NL} \int_{z_l}^{z_{l+1}} \begin{bmatrix} \tau_{xz} \\ \tau_{yz} \end{bmatrix} [1, z^2, z, z^3]$$

After integration, these relations can be written in matrix form, which defines the stress resultant and mid-surface strain relations of the laminated general shell and is given by:

$$\begin{bmatrix} \boldsymbol{N} \\ \boldsymbol{N}^* \\ \boldsymbol{M} \\ \boldsymbol{M}^* \\ \boldsymbol{Q} \\ \boldsymbol{Q}^* \\ \boldsymbol{S} \\ \boldsymbol{S}^* \end{bmatrix} = \begin{bmatrix} \boldsymbol{D}_m & \boldsymbol{D}_c & \boldsymbol{0} \\ \boldsymbol{D}_c^t & \boldsymbol{D}_b & \boldsymbol{0} \\ \boldsymbol{0} & \boldsymbol{0} & \boldsymbol{D}_s \end{bmatrix} \begin{bmatrix} \bar{\boldsymbol{\varepsilon}}_m \\ \bar{\boldsymbol{\varepsilon}}_b \\ \bar{\boldsymbol{\varepsilon}}_s \end{bmatrix} \tag{9a}$$

or symbolically:

$$\bar{\boldsymbol{\sigma}} = \boldsymbol{D}\bar{\boldsymbol{\varepsilon}}$$

in which:

$$\bar{\boldsymbol{\sigma}}^t = (N_x, N_y, N_{xy}, N_x^*, N_y^*, N_{xy}^*, M_x, M_y, M_{xy}, M_x^*, M_y^*, M_{xy}^*, Q_x, Q_y, Q_x^*, Q_y^*, S_x, S_y, S_x^*, S_y^*) \tag{9b}$$

and the stiffness coefficient matrices, i.e. $\boldsymbol{D}_m$, $\boldsymbol{D}_c$, $\boldsymbol{D}_b$ and $\boldsymbol{D}_s$ corresponding to the membrane, coupling between membrane and bending, bending and shear terms, respectively, are defined as follows:

$$\boldsymbol{D}_m = \sum_{l=1}^{NL} \begin{bmatrix} \boldsymbol{Q}_{ij} H_1 & \boldsymbol{Q}_{ij} H_3 \\ \boldsymbol{Q}_{ij} H_3 & \boldsymbol{Q}_{ij} H_5 \end{bmatrix}; \quad \boldsymbol{D}_c = \sum_{l=1}^{NL} \begin{bmatrix} \boldsymbol{Q}_{ij} H_2 & \boldsymbol{Q}_{ij} H_4 \\ \boldsymbol{Q}_{ij} H_4 & \boldsymbol{Q}_{ij} H_6 \end{bmatrix}$$

$$\boldsymbol{D}_b = \sum_{l=1}^{NL} \begin{bmatrix} \boldsymbol{Q}_{ij} H_3 & \boldsymbol{Q}_{ij} H_5 \\ \boldsymbol{Q}_{ij} H_5 & \boldsymbol{Q}_{ij} H_7 \end{bmatrix}; \quad \boldsymbol{D}_s = \sum_{l=1}^{NL} \begin{bmatrix} \boldsymbol{Q}_{lm} H_1 & \boldsymbol{Q}_{lm} H_3 & \boldsymbol{Q}_{lm} H_2 & \boldsymbol{Q}_{lm} H_4 \\ \boldsymbol{Q}_{lm} H_3 & \boldsymbol{Q}_{lm} H_5 & \boldsymbol{Q}_{lm} H_4 & \boldsymbol{Q}_{lm} H_6 \\ \boldsymbol{Q}_{lm} H_2 & \boldsymbol{Q}_{lm} H_4 & \boldsymbol{Q}_{lm} H_3 & \boldsymbol{Q}_{lm} H_5 \\ \boldsymbol{Q}_{lm} H_4 & \boldsymbol{Q}_{lm} H_6 & \boldsymbol{Q}_{lm} H_5 & \boldsymbol{Q}_{lm} H_7 \end{bmatrix} \tag{9c}$$

In the above relations $i, j = 1, 2, 3$ and $l, m = 4, 5$; $H_k = 1/k(z_{l-1}^k - z_l^k)$; $k = 1, 2, 3, 4, 5, 6, 7$; NL is number of layers; and $\bar{\boldsymbol{\varepsilon}} = (\bar{\boldsymbol{\varepsilon}}_m^t, \bar{\boldsymbol{\varepsilon}}_b^t, \bar{\boldsymbol{\varepsilon}}_s^t)^t$ represents the mid-surface membrane, bending and shear strain compo-

nents, respectively, and are defined as follows:

$$\boldsymbol{\varepsilon}_m = \begin{bmatrix} \dfrac{\partial u_0}{\partial x} + \dfrac{w_0}{R_1} + \dfrac{1}{2}\left(\dfrac{\partial w_0}{\partial x}\right)^2 \\ \dfrac{\partial v_0}{\partial y} + \dfrac{w_0}{R_2} + \dfrac{1}{2}\left(\dfrac{\partial w_0}{\partial y}\right)^2 \\ \dfrac{\partial v_0}{\partial x} + \dfrac{\partial u_0}{\partial y} + \dfrac{\partial w_0}{\partial x}\cdot\dfrac{\partial w_0}{\partial y} \\ \dfrac{\partial u_0^*}{\partial y} \\ \dfrac{\partial v_0^*}{\partial x} \\ \dfrac{\partial v_0^*}{\partial x} + \dfrac{\partial u_0^*}{\partial y} \end{bmatrix} ; \boldsymbol{\varepsilon}_b = \begin{bmatrix} \dfrac{\partial \theta_x}{\partial x} \\ \dfrac{\partial \theta_y}{\partial y} \\ \dfrac{\partial \theta_x}{\partial x} + \dfrac{\partial \theta_y}{\partial y} \\ \dfrac{\partial \theta_x^*}{\partial x} \\ \dfrac{\partial \theta_y^*}{\partial y} \\ \dfrac{\partial \theta_x^*}{\partial y} + \dfrac{\partial \theta_y^*}{\partial x} \end{bmatrix} ; \boldsymbol{\varepsilon}_s = \begin{bmatrix} \theta_x + \dfrac{\partial w_0}{\partial x} - \dfrac{u_0}{R_1} \\ \theta_y + \dfrac{\partial w_0}{\partial y} - \dfrac{v_0}{R_2} \\ 3\theta_x^* - \dfrac{u_0^*}{R_1} \\ 3\theta_y^* - \dfrac{v_0^*}{R_2} \\ 2u_0^* - \dfrac{\theta_x}{R_1} \\ 2v_0^* - \dfrac{\theta_y}{R_2} \\ -\dfrac{\theta_x^*}{R_1} \\ -\dfrac{\theta_y^*}{R_2} \end{bmatrix} \tag{10}$$

As the basic equilibrium equation, the virtual work equation for a laminated shell under the assumption of small strain and large displacement in the total Lagrangian coordinate system is considered and can be written in compact form as:

$$\int_A \delta\bar{\boldsymbol{\varepsilon}}^t . \bar{\boldsymbol{\sigma}}\, \mathrm{d}A + \boldsymbol{F}.\delta\boldsymbol{d} = 0 \tag{11}$$

where $\boldsymbol{F}$ is the force vector due to applied forces.

3 C^0 FINITE ELEMENT FORMULATION

The finite element used here is a nine-node isoparametric quadrilateral (Lagrangian family) element. The laminate displacement field in the element can be expressed in terms of the nodal variables as:

$$\boldsymbol{d}(\xi,\eta) = \sum_{i=1}^{NN} \boldsymbol{N}_i(\xi,\eta).\boldsymbol{d}_i \tag{12}$$

where NN is number of nodes per element, $N_i(\xi,\eta)$ contains interpolation functions associated with node i in terms of the local coordinates ξ and η, and $\boldsymbol{d}_i$ is the nodal displacement components vector. The generalized Green strain and its variation vectors, respectively, are $\bar{\boldsymbol{\varepsilon}}$ and $\delta\bar{\boldsymbol{\varepsilon}}$, and these can be expressed in terms of nodal displacement components $\boldsymbol{a}$, displacement gradient $\boldsymbol{\theta}_{NL}$ and cartesian derivatives of shape function matrix $\boldsymbol{N}$ as follows:

$$\bar{\boldsymbol{\varepsilon}} = (\boldsymbol{B}_0 + \tfrac{1}{2}\boldsymbol{B}_{NL})\,\boldsymbol{a} \tag{13a}$$

$$\delta\bar{\boldsymbol{\varepsilon}} = (\boldsymbol{B}_0 + \boldsymbol{B}_{NL})\,\delta\boldsymbol{a} \tag{13b}$$

where $\boldsymbol{B}_0$ is the strain matrix giving linear strains. $\boldsymbol{B}_{NL}$ is linearly dependent upon the nodal dis-

placements $\boldsymbol{a}$ such that $\boldsymbol{a}^t = (\boldsymbol{d}_1^t, \boldsymbol{d}_2^t, \boldsymbol{d}_3^t, \ldots, \boldsymbol{d}_{NN}^t)$ and substituting eqns (12) and (13a, b) in eqn (11), the following discrete equation is obtained:

$$\boldsymbol{K}_0 . \boldsymbol{a} + \boldsymbol{H}(a) . \boldsymbol{a} = \boldsymbol{F} \tag{14}$$

where $\boldsymbol{K}_0$ is a linear elastic stiffness matrix, $\boldsymbol{F}$ is a force vector, and $\boldsymbol{H}(a)$ is a generalized non-linear stiffness matrix which is given by:

$$\boldsymbol{H}(a) = \int_v \boldsymbol{B}_0^t \bar{\boldsymbol{\sigma}}_{NL} \, dA + \int_v \boldsymbol{B}_{NL}^t \bar{\boldsymbol{\sigma}} \, dA \tag{15}$$

where $\bar{\boldsymbol{\sigma}}_{NL}$ is a non-linear stress vector, and the stresses are induced by the non-linear part of the strain.

4 PRESENTATION AND DISCUSSION OF NUMERICAL RESULTS

In order to demonstrate the versatility of the refined theory and C^0 finite elements developed, several examples drawn from the literature are evaluated and discussed. Computer programs have been developed for first-order shear deformation theory (FOST) with five degrees of freedom (u_0, v_0, w_0, θ_x, θ_y) and a higher-order shear deformation theory (HOST) with nine degrees of freedom (u_0, v_0, w_0, θ_x, θ_y, u_0^*, v_0^*, θ_x^*, θ_y^*) per node for both linear and geometrically non-linear analysis of laminated general shells. All the computations were carried out in single precision with a 16-digit word length on CDC Cyber 180/840 computer at the Indian Institute of Technology, Bombay, India.

The results to be discussed are grouped into two categories, viz. (1) linear analysis and (2) non-linear analysis. Since all the shells considered here are either of single layer or of cross-ply laminated shells, only one quadrant of the shell was analyzed using a 2×2 uniform mesh unless otherwise specified. In the present study the nine-node Lagrangian quadrilateral isoparametric element was employed. A selective integration scheme, based on Gauss quadrature rules, viz. 3×3 for integration of membrane, flexure and coupling between membrane and flexure terms, and 2×2 for shear terms in the energy expression, was employed in the evaluation of element stiffness property. All the stress values are reported at the Gauss points nearest to their maximum value locations. A shear correction coefficient of 5/6 is used in FOST.

The material properties, unless otherwise specified, are assumed as:

$$E_1 = 25 \, E_2; \; G_{12} = G_{13} = 0{\cdot}5 \, E_2; \; G_{23} = 0{\cdot}2 \, E_2;$$
$$\nu_{12} = \nu_{21} = 0{\cdot}25; \text{ and}$$
$$E_2 = 10^6 \text{ psi } (214{\cdot}208 \text{ N/mm}^2) \tag{16}$$

Although these properties do not satisfy the symmetry condition, i.e.:

$$\frac{\nu_{12}}{E_1} = \frac{\nu_{21}}{E_2} \tag{17}$$

they are being used here for historical reasons because of their use in many previous studies (see e.g. Pagano;[42] Ren[43] and Kabir[32]).

The finite element displacement formulation developed in this paper is based entirely on assumed displacement functions, and thus only displacement boundary conditions are required to be specified. The boundary conditions corresponding to the present higher-order formulation are specified in Table 1 for different types of supports used in the present investigation.

The corresponding boundary conditions for the first-order shear deformation theory is simply obtained by omitting the higher-order starred (*) displacement quantities. For example there are nine displacement quantities required to be specified at $x = 0, a$ for C type boundary conditions in this higher-order formulation (HOST), whereas in first-order formulation (FOST) the corresponding boundary displacement quantities shall be five only. The boundary condition types S1, S2 and S3 have been especially chosen in order to compare the present authors' results with those of other authors. Incidentally, the S1 type condition corresponds to the usual diaphragm type of simple support. The edge conditions, which have been derived in a variationally consistent manner in the present higher-order theory, may not appear so (except in the case of fully clamped edge specified by C) because, in any way, the natural boundary conditions cannot be prescribed in the displacement based finite element method.

4.1 Linear analysis

4.1.1 Three-layer symmetric cross-ply (0°/90°/0°) laminated plate under sinusoidal transverse load

A simply supported (S1) square cross-ply (0°/90°/0°) laminate subjected to a sinusoidal transverse load is considered. This example is chosen with a view to illustrate the accuracy of the present

Table 1. Boundary conditions

Type	$x=0$		$x=a/2$		$y=0$		$y=b/2$	
S1	$v_0=0$ $\theta_y=0$ $w_0=0$	$v_0^*=0$ $\theta_y^*=0$	$u_0=0$ $\theta_y=0$	$u_0^*=0$ $\theta_y^*=0$	$u_0=0$ $\theta_x=0$ $w_0=0$	$u_0^*=0$ $\theta_x^*=0$	$v_0=0$ $\theta_y=0$	$v_0^*=0$ $\theta_y^*=0$
S2	$u_0=0$ $v_0=0$ $\theta_y=0$ $w_0=0$	$u_0^*=0$ $v_0^*=0$ $\theta_y^*=0$	$u_0=0$ $\theta_y=0$	$u_0^*=0$ $\theta_y^*=0$	$u_0=0$ $v_0=0$ $\theta_x=0$ $w_0=0$	$u_0^*=0$ $v_0^*=0$ $\theta_x^*=0$	$v_0=0$ $\theta_y=0$	$v_0^*=0$ $\theta_y^*=0$
S3	$u_0=0$ $v_0=0$ $w_0=0$	$u_0^*=0$ $v_0^*=0$	$u_0=0$ $\theta_y=0$	$u_0^*=0$ $\theta_y^*=0$	$u_0=0$ $v_0=0$ $w_0=0$	$u_0^*=0$ $v_0^*=0$	$v_0=0$ $\theta_y=0$	$v_0^*=0$ $\theta_y^*=0$
C	$u_0=0$ $v_0=0$ $\theta_y=0$ $\theta_z=0$ $w_0=0$	$u_0^*=0$ $v_0^*=0$ $\theta_y^*=0$ $\theta_z^*=0$	$u_0=0$ $\theta_y=0$	$u_0^*=0$ $\theta_y^*=0$	$u_0=0$ $v_0=0$ $\theta_x=0$ $\theta_z=0$ $w_0=0$	$u_0^*=0$ $v_0^*=0$ $\theta_x^*=0$ $\theta_z^*=0$	$v_0=0$ $\theta_y=0$	$v_0^*=0$ $\theta_y^*=0$

higher-order theory over the first-order theory. The present results are compared with the exact results of 3D elasticity solution given by Pagano.[42] The non-dimensional central deflection and stresses obtained using various theories are compared in Table 2 for different side to thickness ratios.

The present higher-order shear deformation theory results are very close to 3D elasticity results especially from thick-to-moderate-thick zones when compared to first-order shear deformation theory.

The following non-dimensional quantities are used:

$$\hat{w}_0 = \left(\frac{h^3 E_2}{p_0 a^4} \times 100\right) w_0;$$

$$\hat{\sigma}_1 \text{ or } \hat{\tau}_{12} = \left(\frac{h^2}{p_0 a^2}\right)(\sigma_1 \text{ or } \tau_{12}) \tag{18}$$

$$\hat{M} = \left(\frac{1000}{p_0 a^2}\right) M$$

4.1.2 Three-layer symmetric cross-ply (0°/90°/0°) laminated cylindrical shell under sinusoidal transverse load

A symmetric three-ply cylindrical shell of infinite length with radius of 10 in (254 mm), arc length of 10·472 in (265·99 mm) and layers of equal thickness is considered. The material's T direction coincides with the θ direction in the outer layers whilst the material's L direction is parallel to the θ direction in the central layer. A 1×10 ($x \times \theta$ directions) discretization for one-quarter of the shell gives converged results. The transverse displacement $\hat{w}_0$ and the circumferential stresses are taken at the centre of the laminate. The results are presented in Table 3. The following non-dimensional quantities are used to present the results:

$$\hat{w}_0 = \left(\frac{h^3 E_2}{p_0 R^4} \times 10\right) w_0; \quad \hat{\sigma}_\theta = \left(\frac{h^2}{p_0 R^2}\right)(\sigma_\theta) \tag{19}$$

Dennis and Plazotto[14] have adopted a higher-order displacement model which satisfies the shear free boundary condition on the bounding planes of a shell. From the results of Table 3, it is clear that the present higher-order theory predictions are very close to 3D elasticity results in comparison with another higher-order theory and

Table 2. Symmetric cross-ply (0°/90°/0°) square laminate under sinusoidal loading with simply supported (S1) boundaries

a/h	Variable	Pagano[42]	Present	
			FOST	HOST
4	$\hat{w}_0$	–	1·7764	1·9273
	$\hat{\sigma}_1$	0·7550	0·4438	0·7624
	$\hat{\tau}_{13}$	0·0505	0·0371	0·0502
10	$\hat{w}_0$	–	0·6697	0·7181
	$\hat{\sigma}_1$	0·5900	0·5212	0·5929
	$\hat{\tau}_{13}$	0·0289	0·0252	0·0282
20	$\hat{w}_0$	–	0·4925	0·5061
	$\hat{\sigma}_1$	0·5520	0·5393	0·5580
	$\hat{\tau}_{13}$	0·0234	0·0224	0·0232

Table 3. Transverse displacement ($\bar{w}_0$) and extreme fibre circumferential stress ($\hat{\sigma}_\theta$) at the middle of an infinitely long cylindrical shell (0°/90°/0°)

R/h	Variable	Ren[43]	Dennis and Plazotto[44]		Present	
		Exact	HSDT	CST	FOST	HOST
4	$\bar{w}_0$	0·457	0·382 (16·41)	0·078 (82·90)	0·369 (19·26)	0·4086 (10·59)
	$\hat{\sigma}_{\theta b}$	1·772	1·406 (20·65)	0·824 (53·50)	0·827 (53·33)	1·3631 (23·07)
	$\hat{\sigma}_{\theta t}$	1·367	1·117 (18·29)	0·7320 (46·45)	0·729 (46·65)	1·2913 (5·54)
10	$\bar{w}_0$	0·144	0·128 (11·11)	0·0777 (46·04)	0·126 (12·85)	0·1347 (6·46)
	$\hat{\sigma}_{\theta b}$	0·995	0·889 (10·65)	0·7960 (20·00)	0·799 (19·69)	0·8943 (10·12)
	$\hat{\sigma}_{\theta t}$	0·897	0·829 (7·58)	0·7590 (15·38)	0·757 (15·56)	0·8705 (2·95)
50	$\bar{w}_0$	0·081	0·079 (1·49)	0·0776 (3·96)	0·079 (1·58)	0·0800 (1·00)
	$\hat{\sigma}_{\theta b}$	0·798	0·789 (1·13)	0·7920 (0·75)	0·790 (0·79)	0·7924 (0·70)
	$\hat{\sigma}_{\theta t}$	0·782	0·774 (1·02)	0·7740 (1·02)	0·766 (1·99)	0·7724 (1·22)
100	$\bar{w}_0$	0·0787	0·078 (0·76)	0·078 (0·76)	0·078 (0·76)	0·0780 (0·76)
	$\hat{\sigma}_{\theta b}$	0·7860	0·787 (0·13)	0·779 (0·89)	0·795 (1·22)	0·7957 (1·23)
	$\hat{\sigma}_{\theta t}$	0·781	0·770 (1·40)	0·776 (0·64)	0·759 (2·76)	0·7616 (2·48)

Values in parenthesis are percentage differences with respect to the 3D elasticity solution.

first-order shear deformation theory. The higher-order theory presented by Dennis and Plazotto[44] gives stiffer solutions. This may be due to the imposition of shear free conditions on the bounding surfaces. The classical shell theory (CST) predictions are very poor, especially in thick zones.

From the results presented in the preceding sections, it is clear that the present higher-order shear deformation theory gives in general more accurate results in comparison with first-order shear deformation theory and other higher order shear deformation theories based on C^1 continuity.

4.1.3 Cross-ply spherical shell under uniform and sinusoidal loads

To show further the validity of the present formulation, a simply supported (S1) symmetric cross-ply spherical shell with laminations (0°/90°/90°/0°) and (0°/90°/0°) subjected to uniform load and sinusoidal load is considered and the results are compared with 2D closed-form solutions given by Reddy and Liu[16] in Tables 4 and 5. The present results are also compared with closed-form solutions given by Kabir[32] for a symmetric cross-ply (0°/90°/0°) spherical shell with $R/a = 10$ and $a/h = 10$ under different support conditions. These are presented in Table 6, and Fig. 2 shows the variation of displacement with respect to the a/h ratio for a clamped (C) cross-ply (0°/90°/0°) spherical shell of $R/a = 10$. The non-dimensional quantities used here are as given in eqn (18) with $\hat{w}_0 = 10\bar{w}_0$.

From these results it is clear that there is good agreement between the present results and other reliable solutions in thick-to-thin regimes of both shallow-to-deep shells.

4.2 Non-linear analysis

4.2.1 Isotropic shells

A clamped isotropic cylindrical shell with $a = b = 508$ mm, $h = 3{\cdot}175$ mm, $R = 2540$ mm, $E = 3{\cdot}103$ kN/mm^2 and $\nu = 0{\cdot}3$ subjected to uniform load is considered. The present results

Table 4. Transverse displacement ($\bar{w}_0$) for a symmetric cross-ply (0°/90°/0°) spherical shell with simply supported (S1) boundaries

R/a	Theory	Sinusoidal load				Uniform load			
		$a/h = 100$		$a/h = 10$		$a/h = 100$		$a/h = 10$	
		Reddy and Liu[16]	Present	Reddy and Liu[16]	Present	Reddy and Liu[16]	Present	Reddy and Liu[16]	Present
5	FOST	1·0337	1·0310	6·4253	6·4277	1·5118	1·5062	9·794	9·808
	HOST	1·0321	1·0314	6·7688	6·8701	1·5092	1·5066	10·332	10·505
10	FOST	2·4109	2·4077	6·6242	6·6277	3·6445	3·6395	10·110	10·126
	HOST	2·4099	2·4095	7·0325	7·1007	3·6426	3·6421	10·752	10·872
20	FOST	3·6150	3·6149	6·6756	6·6797	5·5473	5·5495	10·191	10·208
	HOST	3·6170	3·6189	7·1016	7·1607	5·5503	5·5556	10·862	10·968
50	FOST	4·2027	4·2054	6·6902	6·6944	6·4827	6·4904	10·214	10·232
	HOST	4·2071	4·2107	7·1212	7·1775	6·4895	6·4987	10·893	10·996
100	FOST	4·3026	4·3059	6·6923	6·6965	6·6421	6·6508	10·218	10·235
	HOST	4·3074	4·3115	7·1240	7·1802	6·6496	6·6596	10·895	10·991
Plate	FOST	4·3370	4·3405	6·6939	6·6972	6·6970	6·7060	10·220	10·234
	HOST	4·3420	4·3462	7·1250	7·1810	6·7047	6·7149	10·889	10·998

Table 5. Transverse displacement ($\bar{w}_0$) for a symmetric cross-ply (0°/90°/90°/0°) spherical shell with simply supported (S1) boundaries

R/a	Theory	Sinusoidal load				Uniform load			
		$a/h = 100$		$a/h = 10$		$a/h = 100$		$a/h = 10$	
		Reddy and Liu[16]	Present	Reddy and Liu[16]	Present	Reddy and Liu[16]	Present	Reddy and Liu[16]	Present
5	FOST	1·0279	1·0251	6·3623	6·3646	1·5358	1·5329	9·825	9·839
	HOST	1·0264	1·0255	6·7865	6·8919	1·5332	1·5333	10·476	10·653
10	FOST	2·4030	2·3993	6·5595	6·5623	3·7208	3·7190	10·141	10·157
	HOST	2·4024	2·4014	7·0536	7·1269	3·7195	3·7220	10·904	11·031
20	FOST	3·6104	3·6094	6·6099	6·6137	5·6618	5·6664	10·222	10·239
	HOST	3·6133	3·6143	7·1237	7·1883	5·6660	5·6738	11·017	11·129
50	FOST	4·2015	4·2030	6·6244	6·6282	6·6148	6·6245	10·245	10·263
	HOST	4·2071	4·2096	7·1436	7·2056	6·6234	6·6347	11·049	11·157
100	FOST	4·3021	4·3041	6·6264	6·6303	6·7772	6·7878	10·249	10·266
	HOST	4·3082	4·3111	7·1464	7·2081	6·7866	6·7985	11·053	11·161
Plate	FOST	4·3368	4·3389	6·6280	6·6310	6·8331	6·8440	10·251	10·267
	HOST	4·3430	4·3460	7·1474	7·2089	6·8427	6·8549	11·055	11·163

Table 6. Symmetric cross-ply (0°/90°/0°) spherical shell under uniform load with $R/a = 10$, $a/h = 10$

Type of support	Displacement ($\bar{w}_0$)			Bending moment ($\bar{M}_1$)		
	Kabir[32]	Present		Kabir[32]	Present	
		FOST	HOST		FOST	HOST
S1	10·53	10·126	10·870	122·55	124·82	123·42
S2	9·17	8·872	9·474	106·78	109·76	107·63
S3	9·17	8·970	9·585	106·79	112·01	109·45
C	4·73	4·542	4·900	35·89	38·84	37·91

are compared with Dhatt[45] and Reddy and Chandrashekhara[39] and are presented in Figs 3a and 3b.

A hinged (immovable) isotropic spherical shell with $R_1 = R_2 = 2540$ mm, $h = 99{\cdot}45$ mm, $a = b = 1569{\cdot}8$ mm, $E = 68{\cdot}95$ N/mm^2 and $\nu = 0{\cdot}3$ is considered and the results are presented in Fig. 3c.

Figures 3a–3c show that for the shells considered, the present results match very well with solutions given by others. The limitation of this comparison is that the shells considered are geometrically thin with negligible shear deformation effects. However, this comparison has certainly proved the validity of the present formulation in the non-linear context.

4.2.2 Nine-layer symmetric cross-ply spherical shell under uniform load

A simply supported (S1) nine-layer symmetric cross-ply (0°/90°/...0°) laminated spherical shell

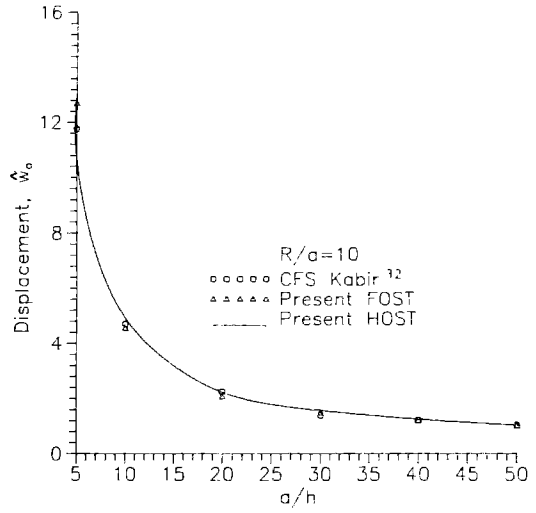

Fig. 2. Displacement versus a/h ratio curve for a cross-ply (0°/90°/0°) laminated spherical shell with clamped (C) supports.

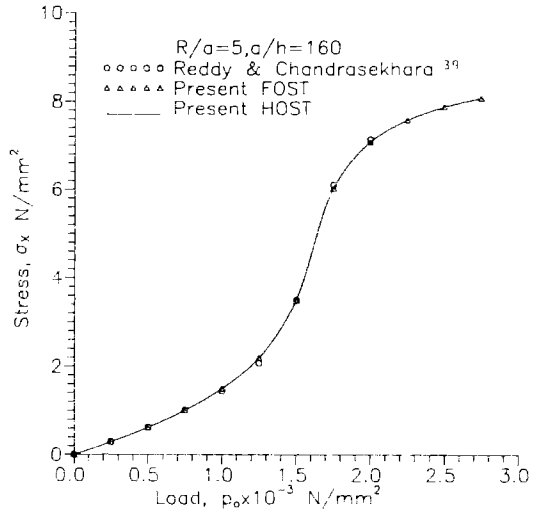

Fig. 3b. Stress versus load curves for a clamped isotropic cylindrical shell under uniform load.

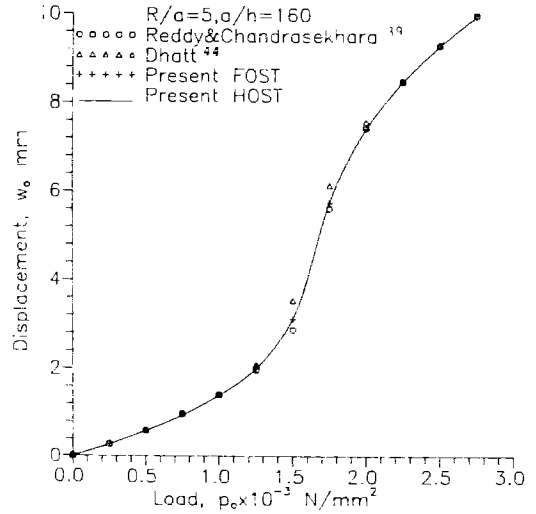

Fig. 3a. Displacement versus load curves for a clamped isotropic cylindrical shell under uniform load.

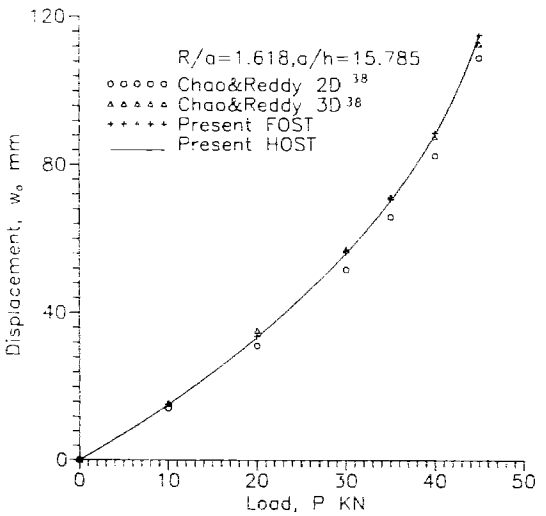

Fig. 3c. Displacement versus load curves for an isotropic spherical shell under crown load with S2 support conditions.

with the following material and geometric data is considered.

$$R_1 = R_2 = 1000 \text{ in } (25{\cdot}4 \text{ m}); \; a = b = 100 \text{ in } (2{\cdot}54 \text{ m}); \; h = 1 \text{ in } (25{\cdot}4 \text{ mm}) \; E_1 = 40E_2; \; E_2 = 10^6 \text{ psi } (214{\cdot}208 \text{ N/mm}^2); \; G_{12} = 0{\cdot}6E_2 \; G_{13} = G_{23} = 0{\cdot}5 \; E_2; \; \nu_{12} = 0{\cdot}25; \; \nu_{21} = 0{\cdot}25 \tag{20}$$

The present HOST results are compared with those given by Noor and Hartley,[36] Chao and Reddy[38] and the present FOST. These are plotted in Fig. 4. The following non-dimensional quantities are used to present the results:

$$\hat{w}_0 = \frac{w_0}{h}; \quad \hat{p}_0 = \frac{p_0}{E_2}\left(\frac{a}{h}\right)^4; \quad \hat{\sigma} = \frac{\sigma}{E_2}\left(\frac{a}{h}\right)^2$$
$$\hat{M} = \left(\frac{10^3}{E_2 a^2}\right) M; \quad \hat{p} = \frac{p}{E_2}\left(\frac{a}{h}\right)^4 \tag{21}$$

The present results agree, in general, with the other investigations. The results given by Noor and Hartley[36] are, however, different from others. The diagnosis is difficult indeed.

4.2.3 Cross-ply spherical shell under uniform and sinusoidal loads

This problem is selected in order to carry out a convergence study by taking 2×2, 3×3 and 4×4 uniform meshes in a quadrant of the shell. Cross-ply symmetric spherical shells of (0°/90°/90°/0°) and (0°/90°/0°) are considered with $a/h = 5$, $R/a = 10$ and simply supported (S1) boundaries subjected to sinusoidal load and uniform load, respectively. The plots for displacement versus load and stress resultant (bending moment) versus load of four-ply and three-ply shells, respectively, are shown in Figs 5a and 5b. Since the variation in results is marginal, it is concluded that a 2×2

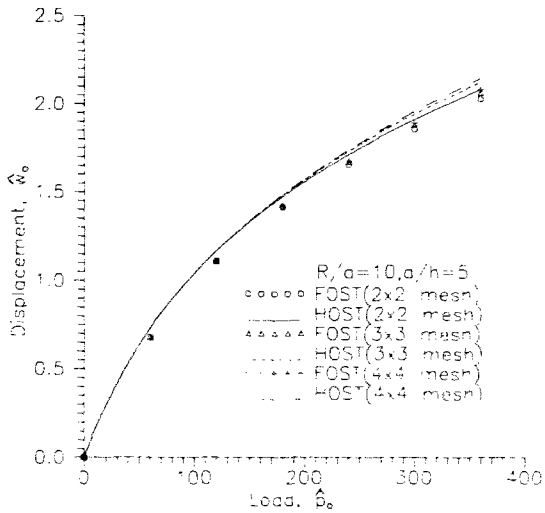

Fig. 5a. Displacement versus load curves for a cross-ply (0/90/90/0) spherical shell under sinusoidal load with S1 boundaries.

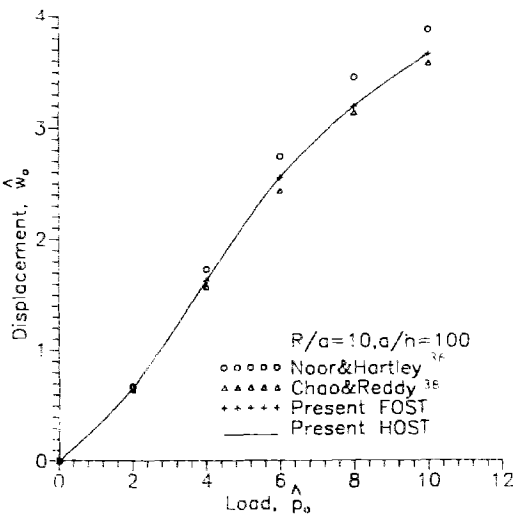

Fig. 4. Displacement versus load curves for a nine-layer cross-ply (0/90/0/ ... /0) spherical shell under uniform load.

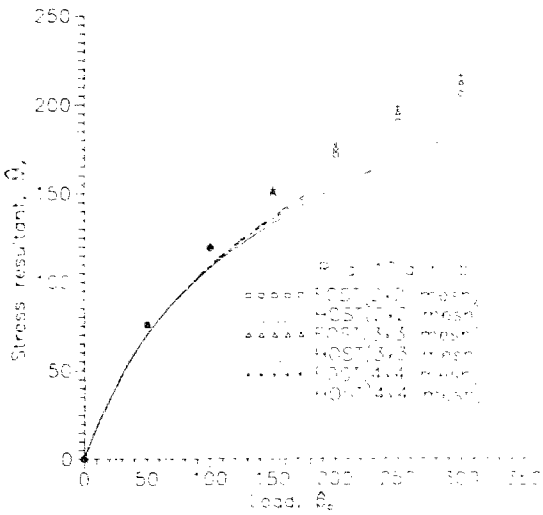

Fig. 5b. Stress resultant versus load curves for a cross-ply (0/90/0) spherical shell under uniform load with S1 boundaries.

mesh gives converged results. The non-dimensional quantities used are as per eqn (21).

4.2.4 Sandwich spherical shell under sinusoidal transverse load

A simply supported (S1) sandwich (0°/90°/core/90°/0°) spherical shell with the following geometrical and material properties is considered:[26]

$a = b = 10$ in (25 mm); $R_1 = R_2 = 10a$

Facings (thickness of each facing layer = 0·05 h)

$E_1 = 1{\cdot}308 \times 10^6$ psi (280·184 N/mm^2);

$E_2 = 1{\cdot}06 \times 10^6$ psi (227·06 N/mm^2)

$\nu_{12} = \nu_{21} = 0{\cdot}28$; $G_{12} = G_{13} = 0{\cdot}6 \times 10^6$ psi (128·525 N/mm^2); and

$G_{23} = 0{\cdot}39 \times 10^6$ psi (83·541 N/mm^2)

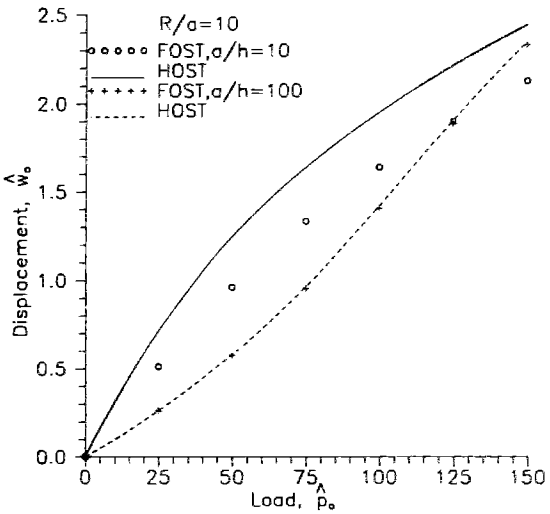

Fig. 6a. Displacement versus load curves for a sandwich spherical shell (0°/90°/core/90°/0°) under sinusoidal transverse load with S1 boundaries.

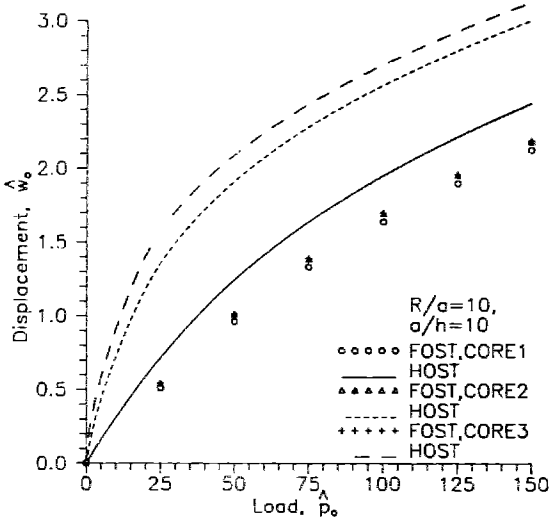

Fig. 6c. Displacement versus load curves for a sandwich spherical shell (0°/90°/core/90°/0°) under sinusoidal transverse load with S1 boundaries.

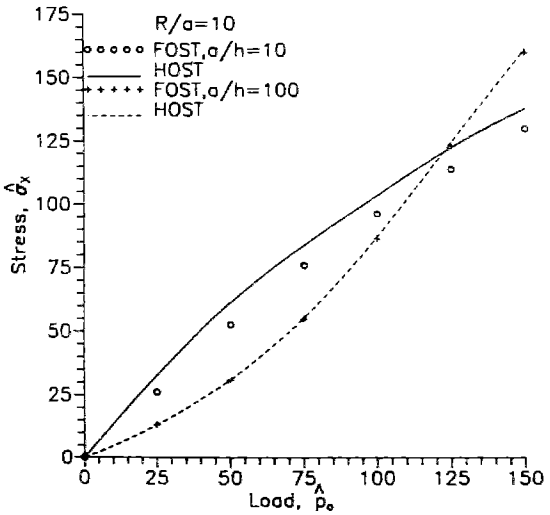

Fig. 6b. Stress versus load curves for a sandwich spherical shell (0°/90°/core/90°/0°) under sinusoidal transverse load with S1 boundaries.

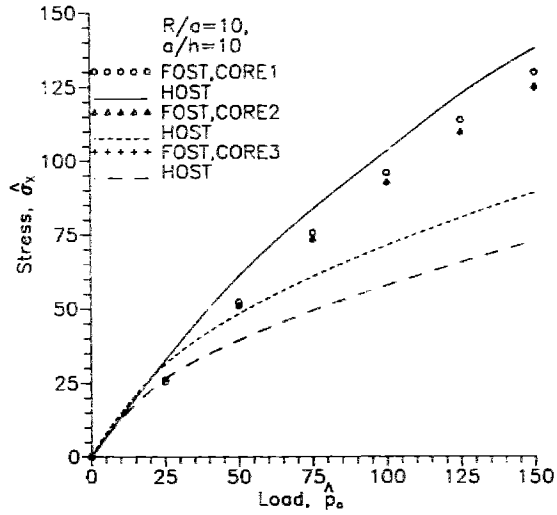

Fig. 6d. Stress versus load curves for a sandwich spherical shell (0°/90°/core/90°/0°) under sinusoidal transverse load with S1 boundaries.

Core (thickness of core = 0·8 h)

Core 1:
$G_{23} = 0{\cdot}1772 \times 10^5$ psi (3·7957 N/mm^2);
$G_{13} = 0{\cdot}5206 \times 10^5$ psi (11·152 N/mm^2)
Core 2:
$G_{23} = 0{\cdot}1772 \times 10^4$ psi (0·37957 N/mm^2);
$G_{13} = 0{\cdot}5206 \times 10^4$ psi (1·1152 N/mm^2)
Core 3:
$G_{23} = 0{\cdot}1772 \times 10^3$ psi (0·03796 N/mm^2),
$G_{13} = 0{\cdot}5206 \times 10^3$ psi (0·11152 N/mm^2)

The shell is subjected to a sinusoidal transverse load. The results for displacements and stresses are presented in Figs 6a–6d. The non-dimensional quantities adopted are as per eqn (21).

From Figs 6a and 6b, it is observed that for $a/h = 100$ the predictions with both higher-order shear deformation theory and first-order shear deformation theory are exactly the same. For $a/h = 10$ considerable difference in the predictions by the two theories is seen. This is due to predominant shear deformation effects in the case of thick sandwich shells.

From the plots Figs 6c and 6d, it is observed that when the core is made progressively weaker the difference between the first-order shear deformation theory and higher-order shear deformation theory predictions for displacements and stresses increases rapidly. In general, the effect is to soften the shell thereby increasing the displacements. It should be noted that there is no variation in the predictions of first-order shear deformation theory for different core properties.

Thus, the first-order shear deformation theory is seen to be inadequate for sandwich shells.

5 CONCLUSIONS

A refined shear flexible C^0 finite element including the effect of geometric non-linearity is employed in the static analysis of laminated general shells. The theory accounts for non-linear variation of transverse shear strains through the thickness and large displacements in the sense of von Karman and therefore no shear correction factors are needed in the present theory.

Numerical results are presented for both linear and geometrically non-linear analysis of composite general shells subjected to various loadings with different edge conditions, laminations, etc.

There is no evidence of availability of 3D elasticity or closed-form 2D non-linear solutions in the literature. It is for this reason that a linear analysis has always been carried out with a view to establish the accuracy of the present formulation by making comparisons with available 3D elasticity solutions.

The present results are very close to the 3D elasticity results both for the thick and thin geometrical configurations.

Due to non-availability of the published data on non-linear behaviour, especially of sandwich shells, an attempt is made here to generate reliable data for future comparisons/evaluations.

It is observed that the effect of shear deformation in moderately thick-to-thick sandwich shells with a weak core and strong facings, and in laminated shells with a large ratio of the tangential elastic modulus to the transverse shear modulus, is considerable. It is believed that the refined higher-order shear deformation theory presented herein is essential for predicting accurate response especially for sandwich shells. The present results may serve as reference results for future investigations.

ACKNOWLEDGEMENT

Partial support of this research by the Aeronautics Research and Development Board, Ministry of Defence, Government of India through Grant Nos. Aero/RD-134/100/10/88/89-518 and Aero/RD-134/100/10/88/89-534 is greatly acknowledged.

REFERENCES

1. Naghdi, P. M., A survey of recent progress in the theory of elastic shells. *Appl. Mechanics Rev.*, **9** (1956) 365–8.
2. Bert, C. W., Analysis of shells. In *Analysis and Performance of Composites*, ed. L. J. Broutman. Wiley Interscience, New York, 1980, pp. 207–58.
3. Ambartsumyan, S. A., Calculation of laminated anisotropic shells. *Izvestia Akademia Nauk Armyanskoi SSR, Ser. Fiz. Mat. Est. Tekh. Nauk*, **6** (1953) 15–23.
4. Ambartsumyan, S. A., *Theory of Anisotropic Shells*. NASA TT F-118, 1964.
5. Hildebrand, F. B., Reissner, E. & Thomas, G. B., Notes on the foundations of small displacements of orthotropic shells. NACA TN-1833, 1949.
6. Naghdi, P. M., On the theory of thin elastic shells. *Quarterly Applied Maths.*, **14** (1957) 369–80.
7. Reissner, E., On a variational theorem in elasticity. *J. Maths & Physics*, **29** (1950) 90–8.
8. Dong, S. B. & Tso, F. K. W., On a laminated orthotropic shell theory including transverse shear deformation. *ASME J. Appl. Mech.*, **39** (1972) 1091–7.
9. Whitney, J. M. & Sun, C. T., A refined theory for laminated anisotropic cylindrical shells. *ASME J. Appl. Mech.*, **41** (1974) 471–6.

10. Widera, G. E. O. & Logan, D. L., Refined theories for non-homogeneous anisotropic cylindrical shells. *ASCE J. Engng Mech.*, **106** (1980) 1053–90.
11. Reddy, J. N., Exact solutions of moderately thick laminated shells. *ASCE J. Engng Mech.*, **110** (1984) 794–809.
12. Kant, T., Thick shells of revolution — some studies. PhD thesis, Department of Civil Engineering, Indian Institute of Technology, Bombay, India, 1976.
13. Kant, T. & Ramesh, C. K., Analysis of thick orthotropic shells. In *Proc. IASS World Congress on Space Enclosures*, Montreal, Canada, 1976, pp. 401–9.
14. Kant, T., A higher-order general shell theory. Research Report C/R/391/81, Civil Engineering Department, University of Wales, Swansea, UK, 1981.
15. Kant, T., A higher-order general laminated shell theory. Research Report, C/R/395/81, Civil Engineering Department, University of Wales, Swansea, UK, 1981.
16. Reddy, J. N. & Liu, C. F., A higher order shear deformation theory of laminated elastic shells. *Int. J. Engng Sci.*, **23** (1985) 319–30.
17. Bhimaraddi, A. & Stevens, L. K., On the higher order theories in plates and shells. *Int. J. Solids & Structures*, **6** (1986) 35–50.
18. Murthy, A. V. K. & Reddy, T. S. R., A higher order theory for laminated composite cylindrical shells. *J. Aeronautical Soc. India*, **38** (1986) 161–71.
19. Kant, T. & Pandya, B. N., A simple finite element formulation of a higher-order theory for unsymmetrically laminated composite plates. *Composite Structures*, **9** (1988) 215–46.
20. Kant, T. & Menon, M. P., Higher order theories for composite and sandwich cylindrical shells with C^0 finite elements. *Computers and Structures*, **33** (1989) 1191–204.
21. Kant, T. & Menon, M. P., Refined multilayered composite cylindrical shell elements. In *Advances in Structural Testing, Analysis and Design*, ed. V. S. Arunachalam *et al.* Proc. Int. Conf. ICSTAD, Tata McGraw Hill, New Delhi, India, 1990, pp. 533–8.
22. Kant, T. & Menon, M. P., Estimation of interlaminar stresses in fibre reinforced composite cylindrical shells. *Computers and Structures*, **38** (1991) 131–47.
23. Kant, T., On finite element discretization of a higher order shell theory. In *Mathematics of Finite Elements and Application*, ed. J. R. Whiteman, Academic Press, London, 1982, pp. 209–17.
24. Kant, T. & Datye, D., Finite elements available for the analysis of curved thin walled structures. In *Finite Element Applications to Thin Walled Structures*, eds. J. W. Bull, Elsevier Applied Science Publishers, London, 1989, pp. 1–40.
25. Kant, T. & Kulkarni, P. B., A C^0 continuous linear beam/bilinear plate flexure element. *Computers and Structures*, **22** (1986) 413–25.
26. Kant, T. & Mallikarjuna, Transient dynamics of composite sandwich plates using 4, 8, 9 noded isoparametric quadrilateral elements. *Finite Elements in Analysis and Design*, **6** (1989) 307–18.
27. Kant, T. & Mallikarjuna, Non-linear dynamics of laminated plates with higher order theory and C^0 finite elements. *Int. J. Non-linear Mechanics*, **26** (1991) 335–43.
28. Kant, T. & Manjunatha, B. S., An unsymmetric FRC laminate C^0 finite element model with 12 degrees of freedom per node. *Engineering Computations*, **5** (1988) 300–8.
29. Kant, T. & Patil, S., Transient/pseudo transient finite element small/large deformation analysis of two dimensional problems. *Computers and Structures*, **36** (1990) 421–7.
30. Mallikarjuna & Kant, T., A general fibre reinforced composite shell element based on a refined shear deformation theory. *Computers and Structures*, **42** (1992) 381–8.
31. Pandya, B. N. & Kant, T., Finite element analysis of laminated composite plates using a higher order displacement model. *Composite Sci. & Technology*, **32** (1988) 137–55.
32. Kabir, H. R. H., Static and dynamic analysis of laminated finite double curved shells. PhD thesis, Department of Civil Engineering, University of Utah, UT, 1990.
33. Horrigmoe, G. & Bergan, P. G., Incremental variational principles and finite element models for non-linear problems. *Computer Methods in Applied Mechanics and Engineering*, **7** (1976) 201–17.
34. Wunderlich, W., Incremental formulations for geometrically non-linear problems. In *Formulations and Algorithms in Finite Element Analysis*, ed. K. J. Bathe, J. T. Oden & W. Wunderlich, US–German Symp. MIT Press, Boston, 1976, pp. 193–239.
35. Stricklin, A., Haisler, W. E. & von Rielsemann, W. A., Evaluation of solution procedures for material and/or geometrical non-linear structural analysis. *AIAA Journal*, **11** (1973) 292–9.
36. Noor, A. K. & Hartley, S. J., Non-linear shell analysis via mixed isoparametric elements. *Computers and Structures*, **7** (1977) 615–26.
37. Chang, T. Y. & Sawamiphakdi, K., Large deformation analysis of laminated shells by finite element method. *Computers and Structures*, **13** (1981) 331–41.
38. Chao, W. C. & Reddy, J. N., Geometrically non-linear analysis of layered composite shells. In *Mechanics of Composite Materials*, ed. G. J. Dvorak, ASME, AMD Vol. 58, New York, 1983, pp. 19–31.
39. Reddy, J. N. & Chandrashekhara, K., Non-linear analysis of laminated shells including transverse shear strains. *AIAA Journal*, **23** (1985) 440–1.
40. Sanders, J. L., An improved first approximation theory for thin shells, NASA TR-24, 1959.
41. Novozhilov, V. V., *Foundations of the Non-linear Theory of Elasticity*, Graylock Press, Rochester, NY, 1953.
42. Pagano, N. J., Exact solutions for rectangular bidirectional composites and sandwich plates. *J. Composite Materials*, **4** (1970) 20–31.
43. Ren, J. G., Exact solutions for laminated cylindrical shells in cylindrical bending. *Composite Sci. & Technol.*, **32** (1987) 137–55.
44. Dennis, S. T. & Plazotto, A. N., Laminated shell cylindrical bending, two dimensional approach vs. exact. *AIAA Journal*, **29** (1991) 647–50.
45. Dhatt, G. S., Instability of thin shells by finite element method. Paper presented at IASS Symp. for Folded Plates and Prismatic Structures, Vienna, 1970.